Biogeosciences Discuss., 12, 13593–13629, 2015
www.biogeosciences-discuss.net/12/13593/2015/
doi:10.5194/bgd-12-13593-2015

Biogeosciences
Discussions

Unusual biogenic calcite structures in two shallow lakes, James Ross Island, Antarctica

J. Elster[1,2], L. Nedbalová[2,3], R. Vodrážka[4], K. Láska[5], J. Haloda[4], and J. Komárek[1,2]

[1]Centre for Polar Ecology, Faculty of Science, University of South Bohemia, Na Zlaté Stoce 3, 37005 České Budějovice, Czech Republic
[2]Institute of Botany, Academy of Sciences of the Czech Republic, Dukelská 135, 37982 Třeboň, Czech Republic
[3]Faculty of Science, Charles University in Prague, Albertov 6, 12843 Prague, Czech Republic
[4]Czech Geological Survey, Klárov 3, 11821 Prague, Czech Republic
[5]Faculty of Science, Masaryk University in Brno, Kotlářská 2, 61137 Brno, Czech Republic

Received: 29 June 2015 – Accepted: 9 August 2015 – Published: 21 August 2015

Correspondence to: J. Elster (jelster@prf.jcu.cz)

Published by Copernicus Publications on behalf of the European Geosciences Union.

Abstract

The floors of two shallow endorheic lakes, located on volcanic surfaces on James Ross Island, are covered with calcareous organosedimentary structures. Their biological and chemical composition, lake water characteristics, and seasonal variability of the thermal regime are introduced. The lakes are frozen down to the bottom eight-nine months per year and their water chemistry is characterized by low conductivity and neutral to slightly alkaline pH. The photosynthetic microbial mat is composed of filamentous cyanobacteria and microalgae that are considered to be Antarctic endemic species. The mucilaginous black biofilm is covered by green spots formed by a green microalga and the macroscopic structures are packed together with fine material. Thin sections consist of rock substrate, soft biofilm, calcite spicules and mineral grains originating from different sources. The morphology of the spicules is typical of calcium carbonate monocrystals having a layered structure and worn surface, which reflect growth and degradation processes. The spicules chemical composition and structure correspond to pure calcite. Lakes age, altitude, morphometry, geomorphological and hydrological stability, including low sedimentation rates, together with thermal regime predispose the existence of this community. We hypothesize that the precipitation of calcite is connected with the photosynthetic activity of the green microalgae that were not recorded in any other lake in the region. This study has shown that the unique community producing biogenic calcite spicules is quite different to any yet described.

1 Introduction

The floors of most Antarctic lakes are covered with photosynthetic microbial mats (Vincent and Laybourn-Parry, 2008). However, the degree of disturbance plays a key role in the development of microbial mats. When growing in low-disturbance habitats, interactions between benthic microbial communities and their environments can produce complex emergent structures on a range of spatial scales. Such structures are best developed in extreme environments, including benthic communities of deep, perennially ice-covered Antarctic lakes, where physical and chemical conditions, and/or geographical isolation preclude larger organisms that could otherwise disrupt organised microbial structures (Wharton, 1994; Andersen et al., 2011). Many organisedimentary structures that emerge in these conditions are laminated and accrete through episodic trapping of sediments or grains and precipitation of minerals within a growing biogenic matrix (e.g. Arp et al., 2001; Reid et al., 2003). In perennially ice-covered lakes, the seasonality of growth imposed by the summer-winter light-dark conditions can induce annual growth laminations (Hawes et al., 2001), reinforced by calcite precipitation during growth and sediment diagenesis (Wharton et al., 1982; Wharton, 1994; Sutherland and Hawes, 2009). Calcite precipitation is not, however, a prerequisite for laminated, stromatolite-like communities (Walter, 1976; Schieber, 1999; Yamamoto et al., 2009).

Precipitation of calcite by expulsion (segregation) is also a common process in the nature related with the freezing of common low ionic strength Ca^{2+} - HCO_3^- waters. Calcite precipitation related to water freezing was observed and described also from various polar-alpine settings, e.g. from lake bottoms of Dry Valleys in Antarctica (Nakai et al., 1975); as a results of aufeis (icing, naled) formation in Northern Canada (Clark and Lauriol, 1997); as crystalline precipitates that form subglacially on bedrock, reported from numerous locations (Ng and Hallet, 2002); as fine-grained calcite powders in subglacial deposits and in aufeis formations, Svalbard (Wadham et al., 2000); in basal ice and subglacial clastic deposits of continental glaciers of Switzerland (Fairchild et al., 1993); as calcite pendants occurring beneath coarse clasts in well-drained sediments, Svalbard (Courty et al., 1994); as calcite coatings in cavities in cold-climate Pleistocene deposits of Western Transbaikalia, Russia, and in modern surface deposits at Seymour Island, Antarctica (Vogt and Corte, 1996); cryogenic calcite powder from modern cave environment (Clark and Lauriol, 1992).

James Ross Island belongs to a transitory zone between the maritime and continental Antarctic regions (Øvstedal and Lewis Smith, 2001). Air temperature records indicate progressive warming trends from 1.5 to 3.0 °C over the Antarctic Peninsula

during the past 50 years (Turner et al., 2014). More than 80 % of the island surface is covered with ice (Rabassa et al., 1982). Only the northernmost part of the island, the Ulu Peninsula, is significantly deglaciated and represents one of the largest ice-free areas in the northern part of the Antarctic Peninsula. The origin of the lakes on James Ross Island is related to the last glaciations of the Antarctic Peninsula ice sheet and retreat of the James Ross Island ice cap during the late Pleistocene and the Holocene (Nývlt et al., 2011; Nedbalová et al., 2013). Interactions between volcanic landforms and glacial geomorphology during previous glacial-interglacial cycles, the Holocene paraglacial and periglacial processes and relative sea level change have resulted in the complex present-day landscape of James Ross Island (Davies et al., 2013). All of these processes have influenced the development of the lakes which are found on the Ulu Peninsula at altitudes from < 20 m above sea level (a.s.l.) near the coast to 400 m a.s.l. in the mountain areas (Nedbalová et al., 2013).

During two Czech research expeditions (2008 and 2009) to James Ross Island, lake ecosystems of the Ulu Peninsula were studied in respect to their origin, morphometry, physical, chemical and biological characteristics (Nedbalová et al., 2013, together with detailed cyanobacterial and microalgal diversity descriptions (Komárek and Elster, 2008; Komárek et al., 2011; Kopalová et al., 2013; Škaloud et al., 2013; Komárek et al., 2015). As part of this study, we encountered 1 to 5 mm scale calcareous organosedimentary structures on the floor of two endorheic lakes, 1 and 2, which are quite different to any microbially mediated structures yet described from modern environments. These shallow lakes on higher-lying levelled surfaces originated after the deglaciation of volcanic mesas which became ice-free some 6.5–8 ka ago (Johnson et al., 2011) and are considered among one of the oldest in the region. However, a later appearance of these lakes is also possible, as we have no exact dates from their sediments (Nedbalová et al., 2013).

The aim of this paper is to describe in detail the chemical and biological composition of the organosedimentary structures (stromatolites sensu Allwood et al., 2006) together with the limnological characteristics of the two lakes. A hypothesis concerning the formation of calcite spicules is also presented. The results of this study can serve as a baseline for understanding microbial behaviors in forming these organosedimentary structures, which will provide insight into the interpretation of fossil forms from early Earth.

2 Materials and methods

2.1 Study site

Endorheic lake 1 (63°54′11.7″ S, 57°46′49.9″ W, altitude 65 m a.s.l.) and endorheic lake 2 (63°53′54.6″ S, 57°46′33.8″ W, altitude 40 m a.s.l.) are shallow lakes located near Andreassen Point on the E coast of the deglaciated Ulu Peninsula, in the northern part of James Ross Island, NE Antarctic Peninsula (Fig. 1). They are shallow with maximum depth of 1.1 and 0.9 m, and mean depth of 0.5 and 0.3 m. Their catchment areas are 340 515 and 368 586 m^2, lake area 4220 and 2970 m^2 and water volume 2183 and 1037 m^3, respectively (Nedbalová et al., 2013). Melt water from the surrounding snowfields feed the lakes for a few weeks during the austral summer. The water level in both lakes fluctuated dramatically. Water is mainly lost through evaporation from the ice free water surface. During this period, intense evaporation in both lakes is coupled with macroscopic changes in the littoral belt (Fig. 2).

Climate conditions of the Ulu Peninsula are characterized by mean annual air temperatures around $-7\,^{\circ}C$ and mean summer temperatures above $0\,^{\circ}C$ for up to four months (Láska et al., 2011a). The mean global solar radiation is around 250 $W\,m^{-2}$ in summer (December-February), with large day-to-day variation affected by extended cyclonic activity in the circumpolar trough and orographic effects over the Antarctic Peninsula (Láska et al., 2011b). The bedrock is composed of two main geological units, namely Cretaceous back-arc basin sediments and mostly subglacial Neogene to Quaternary volcanic rocks (Olivero et al., 1986). The terrestrial vegetation is limited to non-vascular plants and composed predominantly of lichen and bryophyte tundra. A

large number of lakes can be found in this area, formed by glacial erosion and deposition, followed by glacier retreat during the Holocene (Nedbalová et al., 2013).

2.2 Sampling procedures

Lake 1 was sampled on 22 February 2008. In 2009, lake 1 was sampled on 5 January, lake 2 on 12 January. Air temperature at 2 m above ground was measured by an automatic weather station (AWS) located nearby (Fig. 1). Incident global solar radiation was monitored with a LI-200 pyranometer (LI-COR, USA) at Mendel Station, located 11 km northwest of the study site (Fig. 1). The LI-200 spectral response curve covers wavelengths from 400 to 1100 nm with absolute error typically of ±3 % under natural daylight conditions. Global radiation was measured at 10s time interval and stored as 30 min average values, while air temperature was recorded at 1 hour intervals from 1 February 2009 to 30 November 2010. In lake 1, water temperature was monitored from 10 February 2009 to 30 November 2010 at 1 hour intervals using a platinum resistance thermometer with Minikin T data logger (EMS Brno, Czech Republic) installed on the lake bottom.

Conductivity, pH, temperature and dissolved oxygen were measured in situ with a portable meter (YSI 600) at the time the lakes were ice free. Water samples were collected from the surface layer, immediately filtered through a 200 µm polyamide sieve to remove zooplankton and coarse particles. Chlorophyll *a* was extracted from particles retained on Whatman GF/F glass microfiber filters according to Pechar (1987). After centrifugation, chlorophyll *a* was measured by a Turner TD-700 fluorometer equipped with a non-acidification optical kit. The remaining water was kept frozen until analyzed at the Institute of Hydrobiology (Czech Republic). The chemical analytical methods are given in Nedbalová et al. (2013). The stones covered by photoautotrophic mats – biofilm collected in the field were transported to the Czech Republic in a frozen and/or dry state, documented with stereomicroscope (Bresser, HG 424018) and used for (a) phytobenthos community description and isolation of dominant species, (b) fix for thin section analyses, (c) scanning electron and optical microscopy, and (d) determination of the structure and chemical composition of calcium carbonate spicules.

2.3 Thin section analyses

Thin section analyses were made to observe both rock substrate and inorganic particles within biofilms. Dry microbial mat were saturated with epoxy resins in vacuum, subsequently cut perpendicularly and saturated again with epoxy resin. The sample was cemented to a glass slide after grinding and polishing, and a thin section was prepared by final sectioning, grinding and polishing to a desired thickness of 50–55 µm. Thin sections of rocks were studied in transmitted (PPL) and polarized (XPL) light (Olympus BX-51M) and documented in transmitted light of a Nikon SMZ-645 optical microscope using NIS-Elements software.

2.4 Biofilm scanning electron and optical microscopy

The morphology of photoautotrophic mats and calcareous spicules was studied using standard methods of scanning electron microscopy (SEM) using back-scattered electrons (BSE; Jeol JSM-6380, Faculty of Science, Charles University) and optical microscopy (Nikon SMZ-645 using NIS-Elements software). Calcareous spicules were collected directly from the surface of biofilms. Samples studied in SEM were completely dried for 5 months at room temperature, then mounted on stubs with carbon paste and coated with gold prior to photomicrographing.

2.5 Structure and chemical composition of calcium carbonate spicules – EDS and EBSD analyses

The chemical composition of the analyzed spicules was measured by using the Link ISIS 300 system with 10 mm^2 Si-Li EDS detector on a CamScan 3200 scanning electron microscope (Czech Geological Survey, Prague). Analyses were performed using an accelerating voltage of 15 kV, 2 nA beam current, 1 µm beam size and ZAF correction procedures. Natural carbonate standards (calcite, magnesite, rhodochrosite, siderite and smithsonite) were used for standardization. Subsequent structural identification was confirmed by electron backscattered diffraction (EBSD). Identification data and crystallographic orientation measurements were performed on the same scanning electron microscope using an Oxford Instruments Nordlys S EBSD detector. The thick sections used for EBSD applications were prepared by the process of chemo-mechanical polishing using colloidal silica suspension. The acquired EBSD patterns were indexed within Channe l5 EBSD software (Schmidt and Olensen, 1989) applying calcite and aragonite crystallographic models (Effenberger et al., 1981; Caspi et al., 2005). Orientation contrast images were collected from a 4-diodes forescatter electron detector (FSD) integrated into the Nordlys S camera. EBSD pattern acquisition was carried out at 20 kV acceleration voltage, 3 nA beam current, 33 mm working distance and 70° sample tilt.

3 Results

3.1 General description of the lakes and water chemistry

Pictures and detailed bathymetric parameters of both lakes together with marked lines of water level and the maximum extent of the photosynthetic microbial mat littoral belt in lake 1 are presented in Fig. 2.

The physico-chemical characteristics of the lake water for both lakes are given in Table 1. The sampling of lake 1 (pH 7.4–7.9, saturation of oxygen 98.9 %) was performed during cloudy days. Oxygen supersaturation (128 %) together with a relatively high pH (8.6) was observed in lake 2 during a sunny day. Conductivity was below 100 µS cm^{-1} in both lakes. The concentrations of dissolved inorganic nitrogen forms were low, whereas the concentration of dissolved reactive phosphorus (SRP) was 19.3 µg L^{-1} in lake 2. Relatively high concentrations of dissolved organic carbon, particulate nutrients and chlorophyll *a* were also characteristic for lake 2 (Table 1). The autotrophic biomass in lake water was mostly formed by detached benthic species; no substantial phytoplankton developed in the lakes. The comparison of the two sampling dates available for lake 1 suggested high fluctuations of dissolved nutrient concentrations.

3.2 Thermal regime

Fig. 3a shows the annual variation of daily mean water temperature in lake 1 and of daily mean air temperature measured 2 m above ground in the Solorina Valley (locations of air temperature, global radiation and water temperature sensors are marked in Figs. 1 and 2). Lake 1 is frozen to the bottom from the end of March to the end of October or beginning of November. Minimum daily mean winter temperatures on the bottom of the lake were about −12 and −10 °C for 2009 and 2010, respectively. Minimum daily mean air temperatures in the same period were between −32 and −25 °C. Positive summer daily mean water temperatures on the bottom of the lake were between 5 to 9 °C from the beginning of November to the end of March. Air temperatures were frequently lower than water temperatures. Mean monthly water temperatures in the lake ranged from −10.4 (August 2009) to 5.8 °C (February 2010), while monthly mean air temperatures were between −18.7 to 0.7 °C. The differences were greater at the beginning of the winter season (June–July), due to a rapid drop of air temperature.

Diurnal water and air temperature amplitudes in lake 1 and the Solorina Valley are shown in Fig. 3b. The highest night-day air temperature fluctuations (up to 28 °C) were recorded during the winter months, while the lowest, in contrast, occurred in summer. Conversely, the highest night-day amplitudes of water temperature on the bottom of the lake were recorded from November to February, with typical values between 2 and 4 °C.

The course of global solar radiation (Fig. 3c) is smooth, with the maximum daily mean of 385 W m^{-2} during clear sky conditions around the summer solstice. Global radiation reaches the bottom of both lakes during the ice free period.

The relative frequency of hourly values of water temperature at the bottom of lake 1 and air temperature measured 2 m above ground in the Solorina Valley in the period

from 10 February 2009 to 30 November 2010 is shown in Fig. 4. Water temperature fluctuation is narrow, ranging from −15 to 8 °C. This plot also documents that the bottom of the lake is dry frozen, with temperatures from -15° C to most frequently −2 to −6 °C (Fig. 4a). The growing season, with liquid water at temperatures from 2 to 4 °C, covers only two-three months. With respect to air temperature (Fig. 4b), the seasonal thermal regime in the Solorina Valley is much wider (typically from −38 to 8 °C) in comparison with the thermal regime at the bottom of lake 1, where was from −16 up to 8 °C.

The occurrence of days with water temperature higher than −4 °C in lake 1 and monthly mean global solar radiation in the period from February 2009 to November 2010 is shown in Fig. 5. Owing to the variability of the weather conditions, lake water at the bottom is completely frozen only during the coldest one-two months per year (July–August); water temperature is higher than −4 °C in the rest of the year. The water temperature is above 0 °C (liquid phase) from November to April (139 days in average). A number of days with temperature between 0 and −4 °C remains the same as for liquid water occurrence with small changes in the start and end dates towards to the transition period (February–June and September–November, respectively). In such thermal conditions, the benthic littoral community can be metabolically active.

3.3 Littoral phytobenthos – biofilm community description

The littoral benthic community in lakes 1 and 2 are dominated by the heterocytous cyanobacterium *Calothrix elsteri* Komárek 2011, which forms a flat black biofilm on the upper surface of bottom stones (Fig. 6), followed by *Hassallia andreassenni* Komárek 2011 and *Hassallia antarctica* Komárek 2011. *Hassallia andreassenni* is associated with calcium precipitation, as described later. *Hassallia antarctica* was found in stone crevices, being only loosely attached to the substrate. Littoral benthic mats – biofilms on stones are co-dominated on the surface of the blackish cyanobacterial biofilm by the green filamentous and richly-branched alga *Hazenia broadyi* Škaloud et Komárek 2013 (Ulotrichales, Chlorophyceae). *Hazenia broadyi* grew in macroscopic colonies producing green spots (Fig. 6b, d). Later in the summer season, the green spots connected micro fortified mucilaginous lines (Fig. 6c, d). Figure 6a shows the community in early spring whereas Fig. 6b, d originated from later summer when the littoral benthic community was already well developed with a dense coverage of *Hazenia broadyi* green spots. More detailed pictures (Fig. 6e, f) documented the structure of the black leather like biofilm with mucilaginous marble on its surface covered by green spots. When the biofilm gets dry, the net of precipitated micro fortified mucilage mixed with soft mineral particles and crystals of calcium carbonate is visible (Fig. 6g, h).

Scanning electron micrographs document the structure of the biofilm (Fig. 7). Figure 7a shows a lateral view (cross section) of a biofilm with cyanobacterial filaments (*Calothrix elsteri* and *Hassallia andreassenni*). A biofilm upper view (Fig. 7b, d) shows the structure of the cyanobacterial-microalgae community producing the mucilaginous micro fortified net of filaments with spots on its surface.

3.4 Inorganic compounds of biofilms

Thin sections, showing both biofilms and rock substrate (Fig. 8), provided information on various inorganic compounds associated with the soft tissue of the cyanobacterial – microalgal community. These inorganic compounds are represented by (1) allochthonous mineral grains that are overgrown and incorporated by biofilms and (2) calcareous spicules of different sizes ranging from 0.5 mm to 1 cm that are precipitated within the cyanobacterial-microalgal community.

The rock substrate of biofilms is formed by subangular to subrounded pebbles to boulders of basaltic rock, which is dark-grey in colour, compact and usually with a microcrystalline porhyric texture. The rock is not homogenous, but contains numerous ball-like empty voids, which are often partly filled with feldspathoids (Fig. 8a). Crystals of plagioclase (feldspar group) and augite (pyroxene group) are easily recognizable in thin sections (Figs. 8a–c).

Biofilms are often partly covered with various mineral grains and rock fragments, but all specimens studied also contain these particles incorporated directly within soft cyanobacterial – microalgal filaments (Fig. 8a–c).

Mineral grains embedded within biofilms close to the basaltic rock surface are mainly angular to subangular crystal fragments of plagioclase and augite (Figs. 8b, c), i.e. the main mineral components of the basaltic rock substrate described above. In the upper part of biofilms, however, partly or fully incorporated grains of quartz occur, being typically rounded or partly rounded (Figs. 8a, b). One of the thin sections shows a calcareous spicule in situ and mineral grains within the biofilm (Figs. 8c, d).

The structure and morphology of calcareous spicules was studied on SEM (Fig. 9). The spicules (see also Methods) show an intensively worn surface (Fig. 9a), partial or intense recrystallization (Figs. 9a, b) and dissolution (Fig. 9b). Crystal facets on the surface and cleavage (crystallographic structural planes) in the interior of the spicules (Figs. 9a, b) are typical characteristics of calcium carbonate monocrystals.

A non-recrystallized superficial layer of microcrystalline calcite (e.g., Fig. 9b) shows the structure of parallel needle-like calcite microcrystals (Figs. 9d–f). Partial corrosion and dissolution of spicules show distinct layering of these needle-like microcrystals (Fig. 9d). The layered structure of even partly recrystallized spicules is confirmed in the ring-like structures with a cyanobacterial filament in the centre (Fig. 10).

The chemical composition of the studied calcareous spicules determined by FDS corresponds to pure $CaCO_3$. Following chemical composition, calcite and aragonite structural models were applied for the EBSD study focused on structural identification of the crystals forming the spicule. Structural identification of the studied specimen especially prepared for the EBSD study confirmed the absolute agreement between the recorded EBSD patterns and modelled patterns for calcite. The presence of aragonite was not confirmed. FSD images acquired for chemical and orientation contrasts (Fig. 10) show a layered structure especially visible in orientation contrast. This feature reflects continual growing processes on layers with very similar crystallographic orientation. Absolute angular differences between individual layers are below 0.8°.

4 Discussion

4.1 Environmental properties

The Ulu Peninsula is a region of high limnological diversity that is related to differences in lake age, bedrock and altitude. The endorheic lakes under study are characterized by a low content of major ions due to their volcanic bedrock and lower marine influence. In comparison with other lakes of this area, the two lakes show no specific lake water chemistry characteristics with moderate SRP and nitrate concentrations frequently below the detection limit (Nedbalová et al., 2013). High pH together with oxygen supersaturation recorded in lake 2 could be associated with high photosynthetic activity of the mats at the time of sampling.

Because water in either liquid or solid form has a large heat storage capacity, it acts as an important buffer to temperature change. Local climatic conditions of shallow freshwater lakes is the principal external factor controlling their ecological functionality. Lake 1 is frozen to the bottom with minimum daily mean temperatures between −12 and −10 °C approximately eight-nine months per year. For most of the year, however, the temperature of the littoral and lake bottom is only from −2 to −4 °C. In such conditions, a thin layer of water probably covers the surface of the littoral benthic community (the community can be metabolically active at temperatures of about −4 °C) (Davey et al., 1992). The growing season, with liquid water at temperatures between 2 to 4 °C, covers only two-three months.

In regards to heat balance, the studied shallow lakes are pond (wetlands) environments which freeze solid during the winter. This inevitability is a strong habitat-defining characteristic, which places considerable stress on resident organisms (Hawes et al., 1992; Elster, 2002). In summer, they must withstand drying in large parts of the littoral zone due to a considerable drop in water level. In freezing and desiccation resistance studies of freshwater phytobenthos in shallow Antarctic lakes, several ecological measurements have recorded seasonal, diurnal, and year round temperature fluctuations and changes in water state transitions (e.g., Davey, 1989; Hawes et al., 1992,

Hawes et al., 1999). In localities with steady moisture and nutrient supplies, the abundance and species diversity of algae is relatively high. However, as the severity and instability of living conditions increases (mainly due to changes in mechanical disturbances, desiccation–rehydration and subsequent changes in salinity), algal abundance and species diversity decreases (Elster and Benson, 2004). The speed at which water state can change between liquid, ice, and complete dryness, is one of the most important ecological and physiological factors of these lakes. Studies based on field or laboratory experiments have shown that some cyanobacteria and algae are able to tolerate prolonged periods of desiccation. It is also obvious that there are strain/species specific differences in the overwintering strategies, and also between strains/species inhabiting different habitats (Davey, 1989; Hawes et al., 1992; Jacob et al., 1992; Šabacká and Elster, 2006; Elster et al., 2008). The ice and snow which cover the endorheic lakes for about eight-nine months per year serve as a natural incubator which moderate potential mechanical disturbances and stabilise the thermal regimes of the lakes.

4.2 Biodiversity

Patterns of endemism and alien establishment in Antarctica are very different across taxa and habitat types (terrestrial, freshwater or marine; Barnes et al., 2006). Environmental conditions, as well as dispersal abilities, are important in limiting alien establishment (Barnes et al., 2006). Antarctic microbial (cyanobacteria, algae) diversity is still poorly known, although recent molecular and ecophysiological evidence support a high level of endemism and speciation/taxon distinctness (Taton et al., 2003; Rybalka et al., 2009; de Wever et al., 2009; Komárek et al., 2011; Strunecký et al., 2012; Škaloud et al., 2013).

The floors of the studied lakes are covered with photosynthetic microbial mats composed of previously described species of heterocytous cyanobacteria, mostly *Calothrix elsteri* Komárek 2011 followed by *Hassallia andreassenni* Komárek 2011 and *Hassallia antarctica* Komárek 2011 (Komárek et al., 2011). They are co-dominated by a newly described species of green filamentous and richly branched algae *Hazenia* *broadyi* Škaloud et Komárek 2013 (Ulotrichales, Chlorophyceae; Škaloud et al., 2013). All the previously mentioned recently described species have special taxonomic positions together with special ecology and are considered at present as Antarctic endemic species.

The black leather like biofilm with mucilaginous marble on its surface is covered by green spots. These macroscopic structures form mats a few mm thick consisting of the above mentioned species packed in mucilage glued together with fine material. The regular leather biofilm structure with distinct cyanobacterial-microalgal composition and incorporated mineral grains is a modern analogue of some of the oldest well-described Archean stromatolites (sensu Allwood et al., 2006). During the limnological survey of the whole Ulu Peninsula (Nedbalová et al., 2013), this specific biofilm structure was observed only in these two endorheic lakes, although lakes with very similar morphometric and chemical characteristics are found in the area. The mat structure is thus apparently tightly linked to the species composition (Andersen et al., 2011).

The low abundance of benthic diatoms in the lakes is unusual, but not unprecedented as there are other areas in Antarctica where diatoms are scarce or absent (Broady, 1996; Wagner et al., 2004). The reason underlying the absence of diatoms is not immediately obvious, because diatoms are quite a common and frequently dominant component of microbial communities in most freshwater habitats of the Ulu Peninsula, James Ross Island (Kopalová et al., 2013). Local geographical separation of lakes 1 and 2 together with founder effect may have precluded successful colonization by the subset of diatoms that are common in the surrounding freshwater habitats. Although it has long been held that diatoms are dispersed widely, some recent reports document very small scale microbial distributions and endemism (Kopalová et al., 2012; Kopalová et al., 2013).

4.3 Inorganic compounds of biofilms

Based on the character of the rock substrate and lake sediments it is suggested, that one of the main prerequisites for existence of this cyanobacterial-microalgal community

producing unusual biogenic calcite structures is; (1) flat and stable substrate in both lakes and (2) low sedimentation rate.

The substrate for biofilms is composed of boulders and pebbles of the stony littoral zone, petrographically corresponding to compact and massive basaltoids (Smellie et al., 2008; Svojtka et al., 2009). Rounded or sub-rounded quartz grains that are incorporated (“trapped”) within biofilms cannot originate from basaltic volcanic rocks forming the bottom of both lakes and substrate of the studied biofilms. This is evidenced by the petrographic character of the basaltoids, which do not contain any quartz. The presence of abraded quartz grains in lake 1 and 2 can be easily explained by wind transport (e.g., Shao, 2008).

The specific cyanobacterial-microalgal community described above can prosper in the two shallow endorheic lakes, because of low sedimentation rates resulting from minor water input. Low sedimentary input is the main necessary ecological parameter which facilitates the existence of this special microbial community. The community is, however, well adapted to seasonally elevated sedimentation rates coming from frequent and intense winds. During wind storms, the wind is carrying a relatively large amount of small mineral grains and rock microfragments (intense eolic erosion; e.g., Shao 2008 and references therein). These grains and particles are usually derived from erosion of the rocks either in the very close vicinity of the locality (weathering of basaltic rocks), but mainly come from remote locations where especially Upper Cretaceous marine sedimentary sequences are outcropping (Smellie et al., 2008; Svojtka et al., 2009). Even elevated amounts of mineral grains transported into the lake by wind do not stop the growth of cyanobacterial-microalgae biofilms, due to their ability of incorporating and ”trapping” mineral grains within the living tissue.

This study has shown that inorganic substances precipitated by microbial lithogenetic processes are exclusively represented by calcite spicules. Precipitation of carbonate outside of microorganisms during photosynthesis as a mechanism of carbonate construction was described for many filamentous cyanobacterial species (Schneider and Le Campion-Alsumard, 1999). However, the biogenic calcite structures in both lakes are quite different to any microbially mediated structures yet described from modern environments (Kremer et al., 2008; Couradeau et al., 2011). Although there are many lakes with thick mats and similar chemical characteristics on the Ulu Peninsula, the calcite spicules were found exclusively in the two endorheic lakes. We believe that their formation is linked to the specific photoautotrophic mats present in the lakes. From Figs. 6g, h it is clearly visible that the calcareous organosedimentary structures keep contours of viable photosynthetic microbial mat after desiccation or calcite spicules precipitation. More specifically, the co-dominance of a green microalga is unique since mats in Antarctic lakes are most frequently formed by filamentous cyanobacteria (Vincent and Laybourn-Parry 2008). Therefore, we hypothesise that the more rapid photosynthesis rate of *Hazenia* in comparison with cyanobacteria may induce conditions necessary for carbonate precipitation in the lakes (Schneider and Le Campion-Alsumard, 1999; Vincent, 2000). However, abiotic precipitation of calcite is also possible. The segregation of Ca^{2+} and HCO_3^- between ice and the residual solution depend on the freezing rate and hydrogen – oxygen isotope fractionation (O'Neil, 1968; Žák et al., 2004). From our measurements we cannot clearly decide if the winter abiotic calcite precipitation accompany microbial lithogenetic processes.

It is striking that some calcite spicules exhibit recrystallization, forming spicules with the structure of calcite monocrystals. Determining the structure and material of precipitated inorganic substances brought another relevant question: "Do calcite spicules have fossilisation potential"? Microcrystalline calcite forming the recrystallized spicule is a typical material of calcite shells of fossil invertebrates (e.g., Vodrážka, 2009). Although calcite fossils may be partly or completely dissolved during diagenetical processes in the fossil record (e.g., Schneider et al., 2011; Švábenická et al., 2012), their preservation potential is relatively high. Therefore, we expect to find fossil and/or subfossil calcite spicules from the Quaternary lake sediments of the studied area.

Acknowledgements. This study was conducted during two Czech Antarctic research expeditions of the authors (J. Elster, L. Nedbalová, R. Vodrážka, K. Láska, J. Komárek) to the J. G. Mendel station in 2008 and 2009 (headed by Miloš Barták). We are indebted particularly to the staff and scientific infrastructure of the station. The study was supported by the Ministry of Education, Youth and Sports of the Czech Republic (CzechPolar LM2010009 and RVO67985939). R.V. has been funded through a Research and Development Project of the Ministry of Environment of the Czech Republic no. SPII 1a9/23/07 and by a project of the Czech Geological Survey no. 338900. K. Láska was supported by a project of Masaryk University MUNI/A/0902/2012 "Global environmental changes and their impacts" (GlobE). The technical work in laboratories was performed by Jana Šnokhousová and Dana Švehlová.

References

Allwood, A., Walter, M., Kamber, B., Marshall, C., and Burch, I.: Stromatolite reef from the early archaean era of Australia, Nature, 441, 714–718, doi:10.1038/nature04764, 2006.

Andersen, D. T., Sumner, D. Y., Hawes, I., Webster-Brown, J., and McKay, C. P.: Discovery of large conical stromatolites in Lake Untersee, Antarctica, Geobiology, 9, 280–293, doi:10.1111/j.1472-4669.2011.00279.x, 2011.

Arp, G., Reimer, A., and Reitner, J.: Photosynthesis-induced biofilm calcification and calcium concentrations in Phanerozoic oceans, Science, 392, 1701, doi:10.1126/science.1057204, 2001.

Barnes, D. K. A., Hodgson, D. A., Convey, P., Allen, C. S., and Clarke, A.: Incursion and excursion of Antarctic biota: past, present and future, Global Ecol. Biogeogr., 15, 121–142, doi:10.1111/j.1466-822x.2006.00216.x, 2006.

Broady, P. A.: Diversity, distribution and dispersal of Antarctic terrestrial algae, Biodiv. Conserv., 5, 1307–1335, doi:10.1007/BF00051981, 1996.

Caspi, E. N., Pokroy, B., Lee, P. L., Quintana, J. P., and Zolotoyabko, E.: On the structure of aragonite, Acta Crystallogr B, 61, 129–132, doi:10.1107/S0108768105005240, 2005.

Clark, I. D. and Lauriol, B.: Kinetic enrichment of stable isotopes in cryogenic calcites, Chem. Geol., 102, 217–228, doi:10.1016/0009-2541(92)90157-Z, 1992.

Clark, I. D. and Lauriol, B.: Aufeis of the Firth River basin, Northern Yukon Canada: insights to permafrost hydrology and karst, Arct. Alp. Res., 29, 240–252, doi:10.2307/1552053, 1997.

Courty, M. A., Marlin, C., Dever, L., Tremblay, P., and Vachier, P.: The properties, genesis and environmental significance of calcite pendents from the high Arctic (Spitsbergen), Geoderma, 61, 71–102, doi:10.1016/0016-7061(94)90012-4, 1994.

Couradeau, E., Benzerara, K., Moreira, D., Gérard, E., Kaźmierczak, J., Tavera, R., and López-García, P.: Prokaryotic and eukaryotic community structure in field and cultured microbialites from the alkaline lake Alchichica (Mexico), PloS ONE 6, 1–15, doi:10.1371/journal.pone.0028767, 2011.

Davies, B. J., Glasser, N.F., Carrivick, J. L., Hambrey, M. J., Smellie, J. L., and Nývlt, D.: Landscape evolution and ice-sheet behavior in a semi-arid polar environment: James Ross Island, NE Antarctic Peninsula, Special publication, Geological Society of London, doi:10.1144/SP381.1, 2013.

Davey, M. C.: The effect of freezing and desiccation on photosynthesis and survival of terrestrial Antarctic algae and cyanobacteria, Polar Biol., 10, 29–36, 1989.

Davey, M. C., Pickup, J., and Block, W.: Temperature variation and its biological significance in fellfield habitats on a maritime Antarctic island, Antarct. Sci., 4, 383–388, 1992.

De Wever, A., Leliaert, F., Verleyen, E., Vanormelingen, P., Van der Gucht, K., Hodgson, D. A., Sabbe, K., and Vyverman, W.: Hidden levels of phylodiversity in Antarctic green algae: further evidence for the existence of glacial refugee, P. Roy. Soc. B, 276, 3591–3599, doi:10.1098/rspb.2009.0994, 2009.

Effenberger, H., Mereiter, K., and Zemann, J.: Crystal structure refinements of magnesite, calcite, rhodochrosite, siderite, smithsonite and dolomite, with discussion of some aspects of the stereochemistry of calcite-type carbonates, Z. Kristallogr., 156, 233–243, 1981.

Elster, J.: Ecological classification of terrestrial algal communities of polar environment, in: GeoEcology of terrestrial oases, edited by: Beyer, L. and Boelter, M, 303–319, Ecological Studies, Springer-Verlag, Berlin, Heidelberg, 2002.

Elster, J. and Benson, E. E.: Life in the polar terrestrial environment with a focus on algae and cyanobacteria, in: Life In the frozen state, edited by: Fuller, B., Lane, N., and Benson, E. E., Taylor and Francis, London, 111–149, doi:10.1201/9780203647073.ch3, 2004.

Elster, J., Degma, P., Kováčik, L., Valentová, L., Šrámková, K., and Pereira, A. B.: Freezing and desiccation injury resistance in the filamentous green alga Klebsormidium from the Antarctic, Arctic and Slovakia, Biologia, 63, 839–847, doi:10.2478/s11756-008-0111-2, 2008.

Fairchild, I. J., Bradby, B., and Spiro, B.: Carbonate diagenesis in ice, Geology, 21, 901–904, doi:10.1130/0091-7613(1993)021<0901:CDII>2.3.CO;2, 1993.

Jacob, A., Wiencke, C., Lehmann, H., and Krist, G. O.: Physiology and ultrastructure of desiccation in the green alga Prasiola crispa from Antarctica, Bot. Mar., 35, 297–303, doi:10.1515/botm.1992.35.4.297, 1992.

Johnson, J. S., Bentley, M. J., Roberts, S. J., Binnie, S. A., and Freeman, S. P. H. T.: Holocene deglacial history of the northeast Antarctic Peninsula – A review and new chronological constraints, Quaternary Sci. Rev., 30, 3791–3802, doi:10.1016/j.quascirev.2011.10.011, 2011.

Hawes, I., Smith, R., Howard-Williams, C., and Schwarz, A. M.: Environmental conditions during freezing, and response of microbial mats in ponds of the McMurdo Ice Shelf, Antarctica, Antarct. Sci., 11, 198–208, 1999.

Hawes, I., Howard-Williams, C., and Vincent, W. F.: Desiccation and recovery of Antarctic cyanobacterial mats, Polar. Biol., 12, 587–594, 1992.

Hawes, I., Moorhead, D., Sutherland, D., Schmeling, J., and Schwarz, A. M.: Benthic primary production in two perennially ice-covered Antarctic lakes: pattern of biomass accumulation with a model of community metabolism, Antarct. Sci., 13, 18–27, 2001.

Komárek, J. and Elster, J.: Ecological background of cyanobacterial assemblages of the northern part of James Ross Island, NW Weddell Sea, Antarctica, Pol. Polar. Res., 29, 17–32, 2008.

Komárek, J., Nedbalová, L., and Hauer, T.: Phylogenetic position and taxonomy of three heterocytous cyanobacteria dominating the littoral of deglaciated lakes, James Ross Island, Antarctica, Polar Biol., 35, 759–774, doi:10.1007/s00300-011-1123-x, 2011.

Komárek, J., Bonaldo, G. D., Fatima, F. M., and Elster, J.: Heterocytous cyanobacteria of the Ulu Peninsula, James Ross Island, Antarctica, Polar Biol., 38, 475–492, doi:10.1007/s00300-014-1609-4, 2015.

Kopalová, K., Veselá, J., Elster, J., Nedbalová, L., Komárek, J., and Van de Vijver, B.: Benthic diatoms (Bacillariophyta) from seepages and streams on James Ross Island (NW Weddell Sea, Antarctica), Plant Ecol. Evol., 145, 1–19, doi:10.5091/plecevo.2012.639, 2012.

Kopalová, K., Nedbalová, L., Nývlt, D., Elster, J., and Van de Vijver, B.: Diversity, ecology and biogeography of the freshwater diatom communities from Ulu Peninsula (James Ross Island, NE Antarctic Peninsula), Polar Biol., 36, 933–948, doi:10.1007/s00300-013-1317-5, 2013.

Kremer, B., Kaźmierczak, J., and Stal, L. J.: Calcium carbonate precipitation in cyanobacteria mats from sandy tidal flats of the North Sea, Geobiology, 6, 46–56, doi:10.1111/j.1472-4669.2007.00128.x, 2008.

Láska, K., Barták, M., Hájek, J., Prošek, P., and Bohuslavová, O.: Climatic and ecological characteristics of deglaciated area of James Ross Island, Antarctica, with a special respect to vegetation cover, Czech Polar Reports, 1, 49–62, 2011a.

Láska, K., Budík, L., Budíková, M., and Prošek, P.: Method of estimating of solar UV radiation in high – latitude locations based on satellite ozone retrieval with improved algorithm, Int. J. Remote Sens., 32, 3165–3177, doi:10.1080/01431161.2010.541513, 2011b.

Nakai, N., Wada, H., Kiyoshu, Y., and Takimoto, M.: Stable isotope studies on the origin and geological history of water and salts in the Lake Vanda area, Antarctica. Geochem. J., 9, 7–24, 1975.

Nedbalová, L., Nývlt, D., Kopáček, J., Šobr, M., and Elster, J.: Freshwater lakes of Ulu Peninsula, James Ross Island, north-east Antarctic Peninsula: origin, geomorphology, and physical and chemical limnology, Antarct. Sci., 25, 358–372, doi:10.1017/S0954102012000934, 2013.

Ng, F. and Hallet, B.: Patterning mechanisms in subglacial carbonate dissolution and deposition, J. Glaciol., 48, 386–400, 2002.

Nývlt, D., Košler, J., Mlčoch, B., Mixa, P., Lisá, L., Bubík, M., and Hendriks, B. W, H.: The Mendel Formation: evidence for late Miocene climatic cyclicity at the northern tip of the Antarctic Peninsula, Palaeogeogr. Palaeocl., 299, 363–394, doi:10.1016/j.palaeo.2010.11.017, 2011.

Olivero, E. B., Scasso, R. A., and Rinaldi, C. A.: Revision of the Marambio Group, James Ross Island, Antarctica, Instituto Antartico Argentino, Contribución, 331, 1–28, 1986.

O'Neil, J. R.: Hydrogen and oxygen isotope fractionation between ice and water, J. Phys. Chem., 72, 3683–3684, 1968.

Øvstedal, D. O. and Lewis Smith, R. I.: Lichens of Antarctica and South Georgia: A guide to their identification and ecology. Studies in Polar Research, Cambridge University Press, Cambridge, 411 pp., 2001.

Pechar, L.: Use of acetone : methanol mixture for the extraction and spectrophotometric determination of chlorophyll a in phytoplankton., Archiv für Hydrobiologie/Supplement, Algological Studies, 46, 99–117, 1987.

Rabassa, J., Skvarca, P., Bertani, L., and Mazzoni, E.: Glacier inventory of James Ross and Vega Islands, Antarctic Peninsula, Ann. Glaciol., 3, 260–264, 1982.

Reid, P., Dupraz, C., Visscher, P., and Sumner, D.: Microbial processes forming marine stromatolites, in: Fossil and recent biofilms – a natural history of life on Earth, edited by: Krumbein, W. E., Peterson, D. M., and Zavarzin, G. A., Kluwer Academic Publishers, London, 103–118, 2003.

Rybalka, N., Andersen, R. A., Kostikov, I., Mohr, K. I., Massalski, A., Olech, M., and Friedl, T.: Testing for endemism, genotypic diversity and species concepts in Antarctic terrestrial

microalgae of the Tribonemataceae (Stramenophiles, Xanthophyceae), Environ. Microbiol., 11, 554–565, doi:10.1111/j.1462-2920.2008.01787.x, 2009.

Šabacká, M. and Elster, J.: Response of cyanobacteria and algae from Antarctic wetland habitats to freezing and desiccation stress, Polar Biol., 30, 31–37, doi:10.1007/s00300-006-0156-z, 2006.

Shao, Y.: Physics and Modelling of Wind Erosion. Atmospheric and Oceeanographic Sciences Library 37, 2nd Edition, Springer, Heidelberg, 456 pp., 2008.

Schieber, J.: Microbial mats in terrigenous clastics: the challenge of identification in the rock record, Palaios, 14, 3–12, doi:10.2307/3515357, 1999.

Schmidt, N. H. and Olensen, N. O.: Computer-aided determination of crystal-lattice orientation from electron-channeling patterns in the SEM, Can. Mineral., 28, 15–22, 1989.

Schneider, S. and Le Campion-Alsumard, T.: Construction and destruction of carbonates by marine and freshwater cyanobacteria, Eur. J. Phycol., 34, 417–426, doi:10.1017/S0967026299002280, 1999.

Schneider, J., Niebuhr, B., Wilmsen, M., and Vodrážka, R.: Between the Alb and the Alps – The fauna of the Upper Cretaceous Sandbach Formation (Passau region, southeast Germany), Bull. Geosci., 86, 785–816, doi:10.3140/bull.geosci.1279, 2011.

Škaloud, P., Nedbalová, L., Elster, J., and Komárek, J.: A curious occurrence of Hazenia broadyi spec. nova in Antarctica and the review of the genus Hazenia (Ulotrichales, Chlorophyceae), Polar Biol., 36, 1281–1291, doi:10.1007/s00300-013-1347-z, 2013.

Smellie, J. L., Johnson, J. S., McIntosh, W. C., Esser, R., Gudmundsson, M. T., Hambrey, M. J., and Van Wyk de Vries, B.: Six million years of glacial history recorded in volcanic lithofacies of the James Ross Island Volcanic Group, Antarctic Peninsula, Palaeogeogr. Palaeocl., 260, 122–148, doi:10.1016/j.palaeo.2007.08.011, 2008.

Strunecký, O., Elster, J., and Komárek, J.: Molecular clock evidence for survival of Antarctic cyanobacteria (Oscillatoriales,Phormidium autumnale) from Paleozoic times, FEMS Microbiol. Ecol., 82, 482–490, doi:10.1111/j.1574-6941.2012.01426.x, 2012.

Sutherland, D. and Hawes, I.: Annual growth layers as proxies for past growth conditions for benthic microbial mats in a perennially ice-covered Antartic lake, FEMS Microbiol. Ecol., 67, 279–292, doi:10.1111/j.1574-6941.2008.00621.x, 2009.

Švábenická, L., Vodrážka, R., and Nývlt, D.: Calcareous nannofossils from the Upper Cretaceous of northern James Ross Island, Antarctica, Geol. Q., 56, 765–772, doi:10.7306/gq.1053, 2012.

Svojtka, M., Nývlt, D., Muramaki, M., Vávrová, J., Filip, J., and Mixa, P.: Provenance and post-depositional low-temperature evolution of the James Ross Basin sedimentary rocks (Antarctic Peninsula) based on fission track analysis, Antarct. Sci., 21, 593–607, doi:10.1017/S0954102009990241, 2009.

Taton, A., Grubisic, S., Brambilla, E., de Wit, R., and Wilmotte, A.: Cyanobacterial diversity in natural and artificial microbial mats of Lake Fryxell (McMurdo Dry Valleys, Antarctica): a morphological and molecular approach, Appl. Environ. Microb., 69, 5157–5169, doi:10.1128/AEM.69.9.5157-5169.2003, 2003.

Turner, J., Barrand, N. E., Bracegirdle, T. J., Convey, P., Hodgson, D. A., Jarvis, M., Jenkins, A., Marshall, G., Meredith, M. P., Roscoe, H., Shanklin, J., French, J., Goosse, H., Guglielmin, M., Gutt, J., Jacobs, S., Kennicutt, M. C., Valerie Masson-Delmotte, II., Mayewski, P., Navarro, F., Robinson, S., Scambos, T., Sparrow, M., Summerhayes, C., Speer, K., and Klepikov, A.: Antarctic climate change and the environment: an update, Polar Rec., 50, 237–259, doi:10.1017/S0032247413000296, 2014.

Vincent, W. F.: Cyanobacterial dominance in polar regions, in: The Ecology of Cyanobacteria, edited by: Whitton, B. A . and Potts, M., Kluwer Academic Publishers, the Netherlands, 321–340, 2000.

Vincent, W. F. and Laybourn-Parry, J. (Eds.): Polar lakes and rivers, Oxford University Press, Oxford, 346 pp., doi:10.1093/acprof:oso/9780199213887.001.0001, 2008.

Vodrážka, R.: A new method for the extraction of macrofossils from calcareous rocks using sulphuric acid, Palaeontology, 52, 187–192, doi:10.1111/j.1475-4983.2008.00829.x, 2009.

Vogt, T. and Corte, A. E.: Secondary precipitates in Pleistocene and present cryogenic environments (Mendoza Precordillera, Argentina, Transbaikalia, Siberia, and Seymour Island Antarctica), Sedimentology, 43, 53–64, doi:10.1111/j.1365-3091.1996.tb01459.x, 1996.

Wadham, J. L., Tranter, M., and Dowdeswell, J. A.: Hydrochemistry of meltwaters draining a polythermal-based, high-Arctic glacier, south Svalbard: II. Winter and early spring, Hydrol. Process., 14, 1767–1786, doi:10.1002/1099-1085(200007)14:10<1767: AID-HYP103>3.0.CO;2-Q, 2000.

Wagner, B., Cremer, H., Hulzsch, N., Gore, D., and Melles, M.: Late Pleistocene and Holocene history of Lake Terrasovoje, Amery Oasis, East Antarctica, and its climatic and environmental implications, J .Paleolimnol., 32, 321–339, doi:10.1007/s10933-004-0143-8, 2004.

Walter, M.: Stromatolites, Elsevier Science Ltd., Amsterdam, the Nederlands, 790 pp., 1976.

Wharton, R. A., Parker, B. C., Simmons, G. M., and Love, F. G.: Biogenic calcite structures forming in Lake Fryxell, Antarctica, Nature, 295, 403–405, doi:10.1038/295403a0, 1982.

Wharton, R.: Stromatolitic mats in Antarctic lakes, Phanerozoic Stromatolites, II, edited by: Bertrand-Safari, J. and Monty, C., 53–70, Springer, New York, USA, doi:10.1007/978-94-011-1124-9_3, 1994.

Yamamoto, A., Tanabe, K., and Isozaki, Y.: Lower Cretaceous freshwater stromatolites from northern Kyushu, Japan, Paleontol. Res., 13, 139–149, doi:10.2517/1342-8144-13.2.139, 2009.

Žák, J., Urban, J., Cílek, V., and Hercman, H.: Cryogenic cave calcite from several Central European caves: age, carbon and oxygen isotopes and a genetic model, Chem. Geol., 206, 119–135, doi:10.1016/j.chemgeo.2004.01.012, 2004.

Table 1. Physico-chemical characteristics and chlorophyll *a* concentrations in lake water. Samples were collected from surface of lakes. ND – not determined, ANC – acid neutralization capacity, PN – particulate nitrogen, DP – dissolved phosphorus, PP – particulate phosphorus, SRP – dissolved reactive phosphorus, DOC – dissolved organic carbon, PC – particulate carbon, * – laboratory values.

Lake		Green 1		Green 2
Date		22.2.2008	5.1.2009	12.1.2009
Temperature	°C	3.5	ND	12.3
O_2	$mg\,L^{-1}$	13.1	ND	13.7
O_2 saturation	%	98.7	ND	128.0
pH		7.9	7.4*	8.6
Conductivity (25 °C)	$\mu S\,cm^{-1}$	54	48*	97
ANC	$mmol\,L^{-1}$	236	246	455
Na^+	$mg\,L^{-1}$	4.7	5.9	12.5
K^+	$mg\,L^{-1}$	0.24	0.29	0.60
Ca^{2+}	$mg\,L^{-1}$	2.12	1.26	2.32
Mg^{2+}	$mg\,L^{-1}$	1.24	0.77	1.65
SO_4^{2-}	$mg\,L^{-1}$	1.74	1.33	2.60
Cl^-	$mg\,L^{-1}$	5.3	5.1	10.6
NO_3-N	$\mu g\,L^{-1}$	< 5	11	< 5
NO_2-N	$\mu g\,L^{-1}$	0.6	0.2	0.1
NH_4-N	$\mu g\,L^{-1}$	6	< 5	< 5
PN	$\mu g\,L^{-1}$	20	50	73
DP	$\mu g\,L^{-1}$	7.8	20.2	30.4
PP	$\mu g\,L^{-1}$	4.6	5.9	11.7
SRP	$\mu g\,L^{-1}$	4.0	11.6	19.3
DOC	$mg\,L^{-1}$	1.25	1.13	2.17
PC	$mg\,L^{-1}$	0.13	0.41	1.33
Si	$mg\,L^{-1}$	1.45	0.87	2.85
chl *a*	$\mu g\,L^{-1}$	0.9	ND	6.0

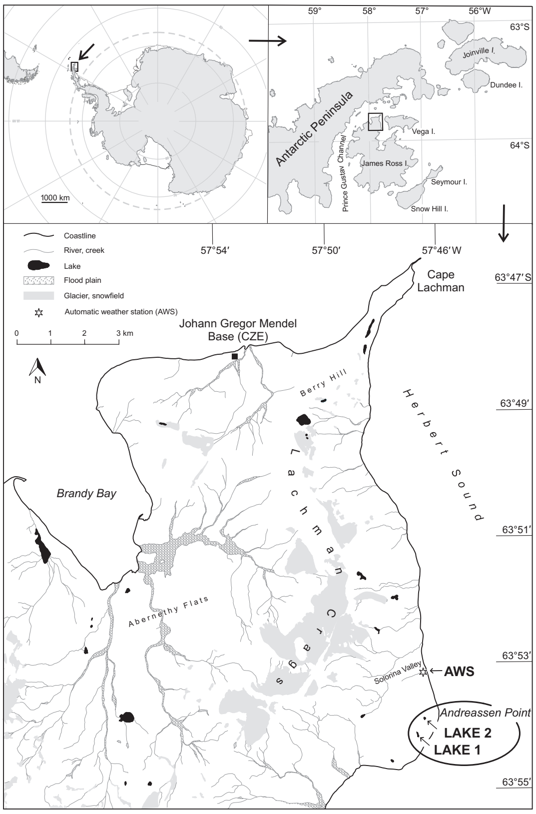

Figure 1. Location of lake 1 and 2 and air temperature measurements (ASW) in the Solorina Valley.

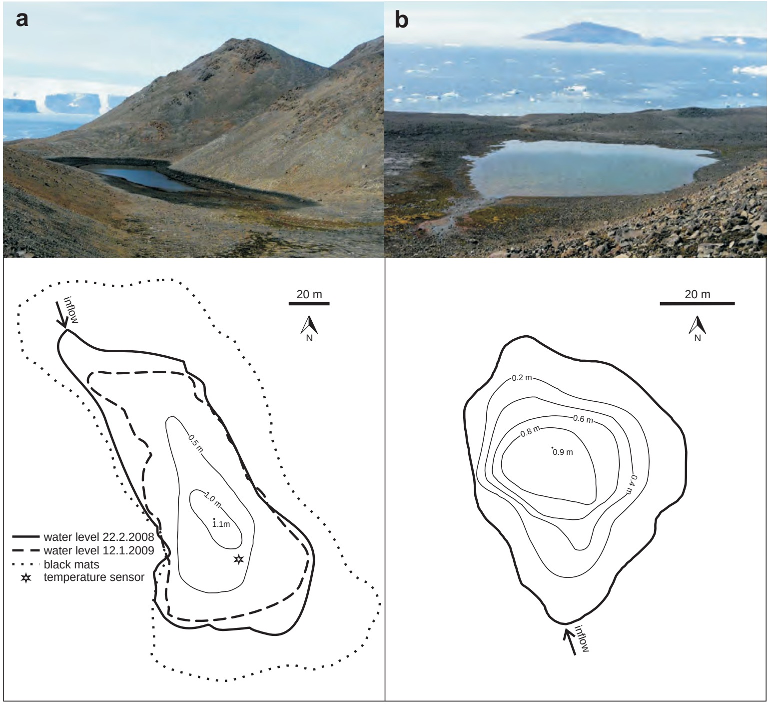

Figure 2. Bathymetric parameters of lake 1 **(a)** and 2 **(b)** together with marked lines of water level and maximum extent of the photosynthetic microbial mat littoral belt in lake 1.

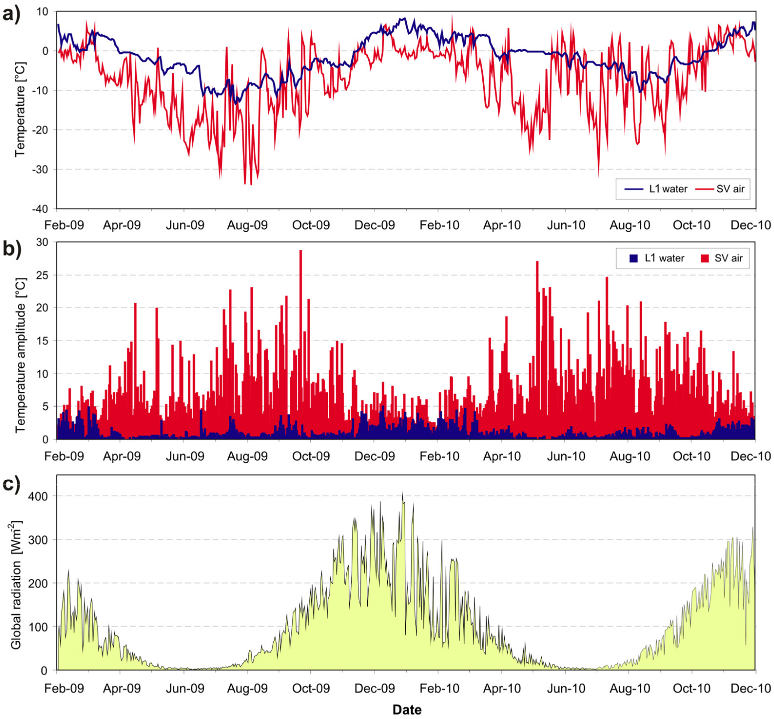

Figure 3. (a) Annual variation of daily mean water temperature in lake 1 (L1water) and annual variation of daily mean air temperature 2 m above ground in the Solorina Valley (SV air), **(b)** Diurnal temperature amplitudes in lake 1 (L1 water) and diurnal air temperature amplitudes in the Solorina Valley (SV air), respectively. **(c)** Daily mean global radiation at Mendel Station. All parameters measured from February 2009 to November 2010.

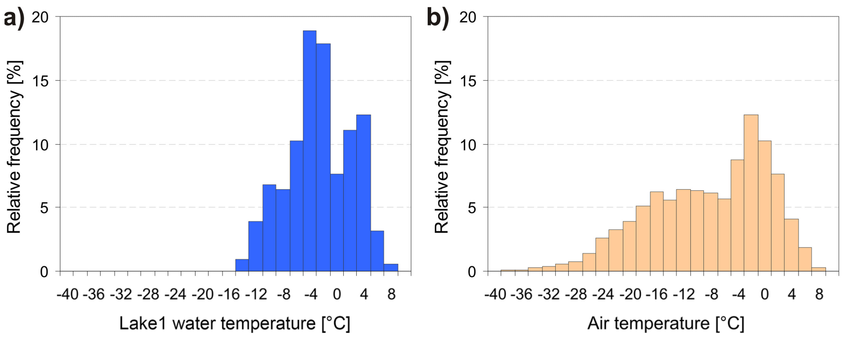

Figure 4. Relative frequency of hourly values of water temperature in lake 1 **(a)** and air temperature measured 2 m above ground in the Solorina Valley **(b)** from February 2009 to November 2010.

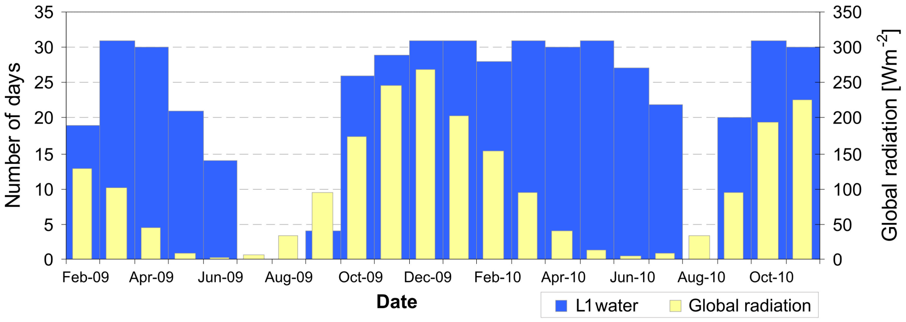

Figure 5. Occurrence of days with lake 1 water temperature (L1 water) higher than −4 °C complemented with monthly mean global solar radiation at Mendel Station both from February 2009 to November 2010.

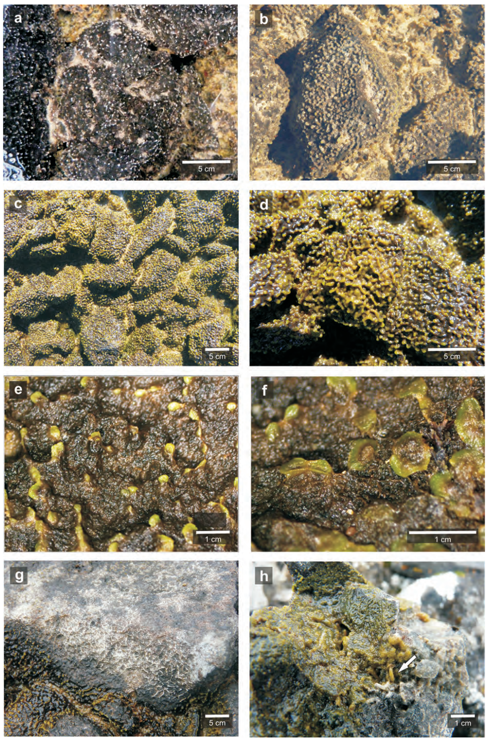

Figure 6. Photoautotrophic mats in lakes 1 and 2. **(a)** Rapid development of the mat in January 2009 (lake 1). The two photos show the mat at a one week interval, note the growth of gelatinous clusters of densely agglomerated filaments of the green alga *Hazenia broadyi*, **(c, d)** fully developed mats with mosaic-like structures on the surfaces of stones in the littoral zone of lake 2, **(e, f)** detail, **(g)** drying of the mat in the littoral zone leaves a characteristic structure on the surface of stones, **(h)** calcium carbonate spicule in situ (arrowed).

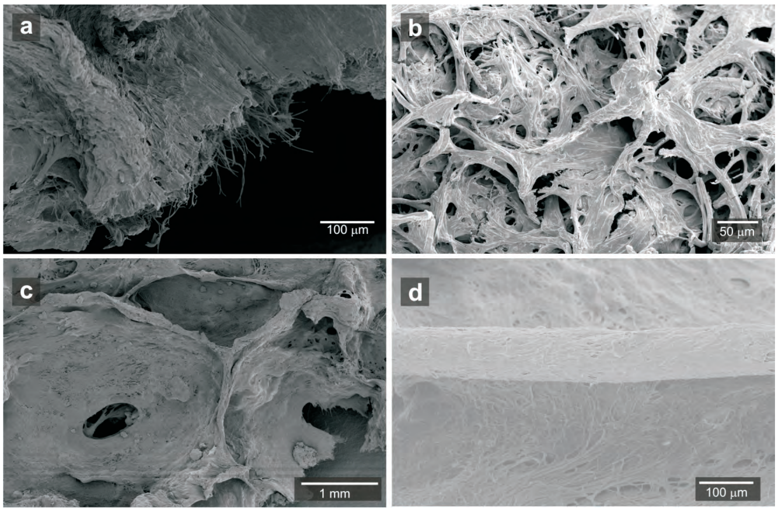

Figure 7. SEM macrographs showing the structure of the dried mat in the lakes. **(a)** Transversal section of the mat with visible cyanobacterial filaments, **(b)** surface structure of the mat, **(c)** general view of the surface structure of the mat with the net formed by mucilage (compare with Fig. 7d), **(d)** detail of the same mucilaginous structure.

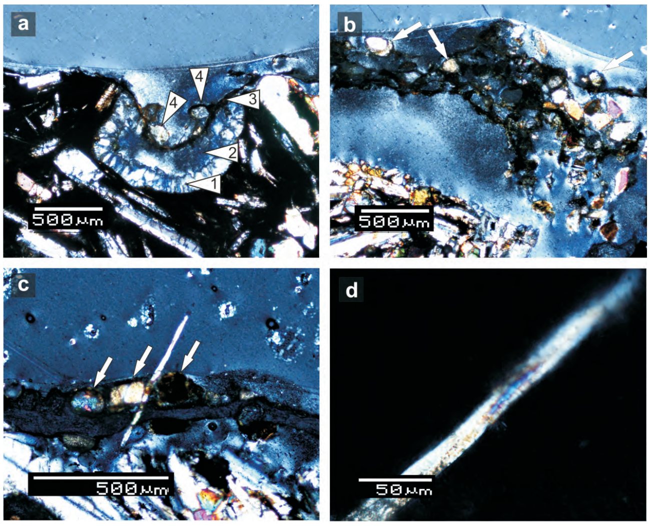

Figure 8. Perpendicular thin sections of rock substrate overgrown by biofilms. Note that biofilms are partly detached from the surface of the rock due to complete drying of the sample. **(a)** Conspicuous U-shaped empty void (arrowed "2") near the surface of basaltic rock partly infilled with crystals of feldspathoids (tectosilicate minerals, arrowed "1"); empty void is bridged by biofilm (arrowed "3") with partly incorporated mineral clasts, represented by semi-rounded quartz grains (arrowed "4"), **(b)** rather thick biofilm with numerous incorporated mineral grains. Note that close to the rock substrate the angular grains of plagioclase (feldspar group) and augite (pyroxene group) dominate, being derived from basaltoids, whereas close to the surface rounded grains of quartz occur (arrowed), **(c)** in situ calcium carbonate spicule penetrating biofilm and surrounded by incorporated grains of feldspars (two arrows on the left) and pyroxene (arrow on the right), **(d)** close up of the same calcium carbonate spicule with a cyanobacterial filament in its centre.

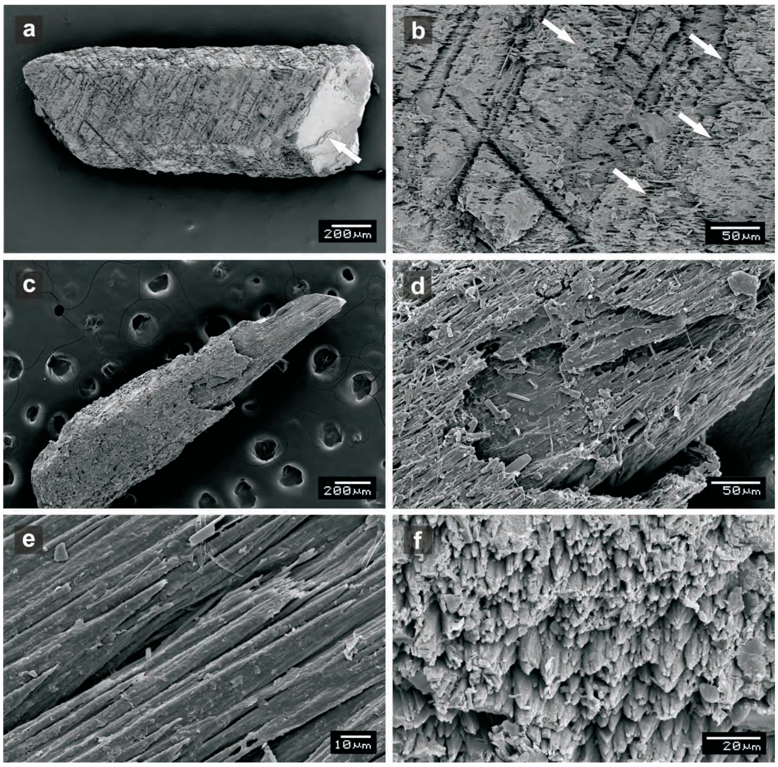

Figure 9. SEM macrographs showing the morphology of partly recrystallized calcium carbonate spicules. Spicules were washed away from the living tissue and collected directly from the surface of biofilms, although residence time on the bottom cannot be determined. **(a)** Calcareous spicule showing intensively worn surface and complete recrystallization of the spicule interior. The spicule shows crystal facets on the surface and cleavage (crystallographic structural planes) in the interior (arrowed) – i.e. typical characteristics of calcium carbonate monocrystal, **(b)** detail of previous image; two parallel systems of deep furrows on the surface are crystallographic structural planes of calcite monocrystal; remnants of a superficial layer of microcrystalline calcite are, however, preserved in places on the surface of the crystal (arrowed), **(c–f)** poorly recrystallized spicule, formed mainly by microcrystalline calcite, **(c)** lateral view of the spicule, **(d)** detail of the surface showing corrosion of needle-like calcite microcrystals with distinct layering, **(e)** parallel needle-like calcite microcrystals on the surface of the central part of the spicule, **(f)** tops of parallel needle-like calcite microcrystals on the surface of the terminal part of the spicule; the view is perpendicular with respect to the previous macrograph.

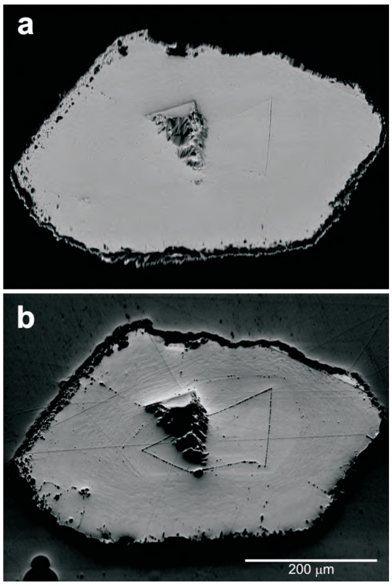

Figure 10. FSD image of a transversely sectioned, partly recrystallized calcite spicule acquired in **(a)** chemical contrast, **(b)** orientation contrast.